Crucial roles of Brn1 in distal tubule formation and function in mouse kidney

Shigeyasu Nakai[1,6], Yoshinobu Sugitani[1], Hiroshi Sato[2], Sadayoshi Ito[2], Yukio Miura[3], Masaharu Ogawa[4], Miyuki Nishi[1], Kou-ichi Jishage[1], Osamu Minowa[1,5] and Tetsuo Noda[1,5,6,*]

[1]Department of Cell Biology, Japanese Foundation for Cancer Research (JFCR) Cancer Institute, 1-37-1 Kami-Ikebukuro, Toshima-Ku, Tokyo 170-8455, Japan
[2]Division of Nephrology, Endocrinology, and Vascular Medicine, Tohoku University School of Medicine, Sendai 980-8574, Japan
[3]Miyagi Insurance Hospital, Sendai 981-1103, Japan
[4]Laboratory for Cell Culture Development, Brain Science Institute, RIKEN, Wako, Saitama 351-0198, Japan
[5]Mouse Functional Genomics Research Group, RIKEN Genomic Sciences Center, Kanagawa 244-0804, Japan
[6]Division of Molecular Genetics, Center for Translational and Advanced Animal Researches on Human Diseases, Tohoku University School of Medicine, Sendai 980-8575, Japan
*Author for correspondence (e-mail: tnoda@ims.u-tokyo.ac.jp)

Accepted 12 June 2003

Development 130, 4751-4759

doi:10.1242/dev.00666

Summary

This study identifies a role for the gene for the POU transcription factor Brn1 in distal tubule formation and function in the mammalian kidney. Normal development of Henle's loop (HL), the distal convoluted tubule and the macula densa was severely retarded in *Brn1*-deficient mice. In particular, elongation and differentiation of the developing HL was affected. In the adult kidney, Brn1 was detected only in the thick ascending limb (TAL) of HL. In addition, the expression of a number of TAL-specific genes was reduced in the *Brn1*$^{+/-}$ kidney, including *Umod*, *Nkcc2*/*Slc12a1*, *Bsnd*, *Kcnj1* and *Ptger3*. These results suggest that Brn1 is essential for both the development and function of the nephron in the kidney.

Key words: Brn1, Henle's loop, Kidney, Distal tubule formation, POU transcription factor

Introduction

Mammalian kidney development is initiated by the reciprocal interaction of two primordial mesodermal derivatives: the ureteric bud and the metanephric mesenchyme. First, the ureteric bud is induced from the mesonephric (Wolffian) duct by the metanephric mesenchyme, then the metanephric mesenchyme near the bud is transformed to form the renal vesicle, a spherical cyst consisting of early epithelial cells. Through a series of invaginations and elongations, this cyst finally develops into the mature nephron, which is a minimally functional filtration unit central to kidney function (Kuure et al., 2000; Schedl and Hastie, 2000). The mammalian kidney contains many nephrons, each consisting of a glomerulus and tubules. The glomerulus acts to filter the plasma and the tubules, which are divided into proximal, intermediate and distal, function to reabsorb water and small molecules such as ions from the filtrate (Bachmann and Kriz, 1998). Among the nephron tubules, Henle's loop (HL) has a unique structure and is essential for hypertonic urine production, which conserves water and ions to maintain homeostasis in the body (Greger, 1985). Although a number of molecules including transcription factors and growth factors have been implicated by genetic screens in the early phases of mammalian kidney development, the mechanisms controlling the unique and complex nephron patterning remain to be elucidated (Kuure et al., 2000; Schedl and Hastie, 2000). This patterning is a key process for the establishment of kidney function later in development.

Transcription factors are essential for the development of complex organ systems. POU transcription factors, which carry a common DNA binding motif called a POU domain, regulate a variety of developmental processes. Brn1 (Pou3f3 – Mouse Genome Informatics) and Brn2 (Pou3f2 – Mouse Genome Informatics) are members of the class III family of mammalian POU transcription factors, and share extremely high sequence homology within the POU domain. They are both prominently expressed in the central nervous system during embryonic development (He et al., 1989). These two factors show a high level of redundancy, as targeted mutagenesis of either of these genes only leads to changes in very restricted regions of the brain. Brn1-deficient mice die within 48 hours of birth, but show histological abnormalities only in the hippocampus region (data not shown), which are not sufficient to explain their postnatal death. Analysis of the *Brn1*/*Brn2* double mutants showed that Brn1 and Brn2 regulate the production and positioning of neocortical neurons (McEvilly et al., 2002; Sugitani et al., 2002), but the cause of death in the Brn1-deficient mice remains unclear.

Brn1, but not Brn2 or any other class III POU proteins, is also expressed in the developing kidney of rat embryos, but its function here remains unknown (He et al., 1989). We describe, in detail, our analysis of the spatial and temporal patterns of Brn1 expression in the developing mammalian kidney. Histological and functional changes to the kidney in Brn1-mutant mice were also analyzed. The results clearly suggest that Brn1 may play an essential role not only in the formation of the HL, distal convoluted tubule (DCT) and macula densa

(MD) structure in the developing kidney, but also in the function of the thick ascending limb (TAL) of HL in the adult kidney.

Materials and methods

Generation of *Brn1*$^{-/-}$ mice

To construct the targeting vector, we used Lambda DASH II phage clones isolated from a 129/SV mouse genomic library. A 9 kb *Not*I-*Not*I fragment derived from the 5′ region of *Brn1* and a 1.3 kb *Apa*I-*Apa*I fragment from the 3′ region were used as homologous flanking sequences. A 1.2 kb pGK-neo cassette was inserted at the 3′-end of the right arm for positive selection. Linearized plasmid DNA was electroporated into J1 ES cells as described (Nakai et al., 1995). Of 700 G418-resistant colonies, we identified eleven properly targeted clones as determined by Southern blot analysis. Two independent ES cell clones were microinjected into C57BL/6J blastocysts, resulting in the birth of male chimeras. Germline transmission of the disrupted *Brn1* allele was achieved by mating with C57BL/6J females.

Antibodies

A polyclonal anti-Brn1 antibody was generated by immunizing a rabbit with the synthetic polypeptide, PDDVYSQVGIVSAD, corresponding to amino acids 469-482 of mouse Brn1. The specificity of the Brn1 antibody was confirmed by western blot analysis (Fig. 1B), which was performed as previously described (Yao et al., 2002).

Electrophoresis mobility-shift assay (EMSA)

EMSA experiments were performed as previously described (Nakai et al., 1995).

Histology, immunohistochemistry and electron microscopy

For light microscopy, organs were fixed in Bouin's fixative, embedded in paraffin wax and sectioned. Kidney morphology was visualized using 6 μm longitudinal or coronal sections stained with either Hematoxylin and Eosin or periodic acid-Schiffs (PAS). For Brn1 immunohistochemistry, organ samples were fixed in 4% paraformaldehyde (PFA) overnight. Cryostat sections of 10 μm thickness were cut then incubated with anti-Brn1 antibody overnight. Signals were visualized using a Vectastain ABC kit (Vector Laboratories), counterstained with kernechtrot, dehydrated and mounted on glass slides. For Caspase 3, phosphorylated MAPK (ERK1/2), and Bcl2 immunohistochemistry, organ samples were fixed in 4% paraformaldehyde (PFA) overnight. Paraffin wax embedded sections were cut (6 μm) then incubated with anti-cleaved caspase-3 antibody (Asp175) (Cell Signaling Technology) or anti-phosphorylated MAPK (ERK1/2) antibody (Cell Signaling Technology) or anti-Bcl-2 antibody (BD PharMingen) overnight. Signals were visualized using a Vectastain ABC kit (Vector Laboratories), counterstained with Hematoxylin, dehydrated, and mounted on glass slides. For electron microscopy, tissues were fixed in 2% PFA/1% glutaraldehyde in 0.1 M phosphate buffer and embedded in Epon 812 resin. Semi-thin sections (1 μm) were used for Toluidine Blue staining, while ultrathin sections were prepared for examination in a transmission electron microscope.

Cell proliferation assay

E16.5 timed-pregnant heterozygous females were injected intraperitoneally with BrdU (Amersham) at 100 mg kg^{-1} of body weight. Approximately 3 hours after injection, females were sacrificed and the embryos recovered. Kidneys dissected from the embryos were fixed in Bouin's fixative, embedded in paraffin wax and sectioned longitudinally at a (6 μm). Sections were then incubated with anti-BrdU antibody (Becton Dickinson) diluted 1:100 overnight at 4°C. Signals were visualized using a Vectastain ABC kit. Following counterstaining with Hematoxylin, samples were dehydrated and mounted. Three animals for each genotype were subjected to analysis. Total and stained cells were counted in at least four independent Henle's loops to give a percentage of BrdU-positive cells. The average percentage for each animal was then subjected to statistical analysis.

TUNEL assay

Kidneys were dissected from newborn mice, fixed in 10% neutral formalin and embedded in paraffin wax. Sections were cut at 6 μm and subjected to a TUNEL assay. The labeling of fragmented nuclear DNA with terminal deoxynucleotide transferase (Tdt) was performed using an ApopTag Peroxidase Kit (Interogen).

In situ hybridization (ISH)

Organs were fixed in 4% PFA overnight. In situ hybridization of 10 μm cryostat sections was performed as described (Minowa et al., 1999). Riboprobes were synthesized using the following mouse cDNAs: *Ptger3* (10-364), *Umod* (625-932), *Nkcc2* (Slc12a1 – Mouse Genome Informatics) (3086-3331), *Ncc* (360-741), *Ncx1* (Slc8a1 – Mouse Genome Informatics) (442-808), *βENaC* (Scnn1b – Mouse Genome Informatics) (658-976) and *Nos1* (167-516).

RNase protection assay (RPA)

mRNA levels were measured using an RPA as previously described (Nakai et al., 1995). ^{32}P-labeled riboprobes were generated from the cDNAs described above for use in in situ hybridization. The mouse cDNAs of *Bsnd* (203-688), *Egf* (1084-1546), *Clcnk1l* (844-1322), and *Kcnj1* (124-511) were also used for RPA. A plasmid containing ~100 bp of the mouse *Gapd* cDNA was a kind gift from Dr A. Orimo (Saitama Medical School, Iruma, Saitama). The intensities of the radioactive protected bands were quantified on an Image Analyzer (Fuji Film). Test signals were normalized to the *Gapd* signal for each sample. The ratios of observed to wild-type signal were then calculated.

Clinical chemistry

For newborn mice, blood samples were collected by decapitation, while urine samples were collected by forced voiding. In adult mice, blood was collected retro-orbitally using capillary tubes. Urine samples were collected by spontaneous voiding. Serum urea nitrogen levels were measured using a UN-B Test Wako (Wako). Serum creatinine and electrolyte concentrations were measured using DriChem (Fuji Film). Serum and urine sample osmolalities were measured using a Fiske Osmometer Model 110 (Fiske Associates). To determine the daily urine output, mice were kept in metabolic cages under euhydrated conditions.

Glomerular maturity index and glomerular counts

Six newborn animals for each genotype were analyzed. The glomerular maturity index was calculated as described previously (Niimura et al., 1995). The maturity index determined for each animal was an average of the score for all glomeruli present in a median longitudinal section. The total number of glomeruli was also quantitated in a median longitudinal section for each animal.

Results

Homozygous *Brn1*-mutant mice died within 24 hours of birth because of renal failure

To generate *Brn1* knockout mice, a 1.2 kb genomic region that included the translation initiation site and 70% of the *Brn1*-coding region was replaced with *PGK-neo*^{r} contained within the targeting vector (Fig. 1A). Genotyping of F2 offspring generated by double heterozygous breeding identified the expected Mendelian frequency (24.5%) of homozygous

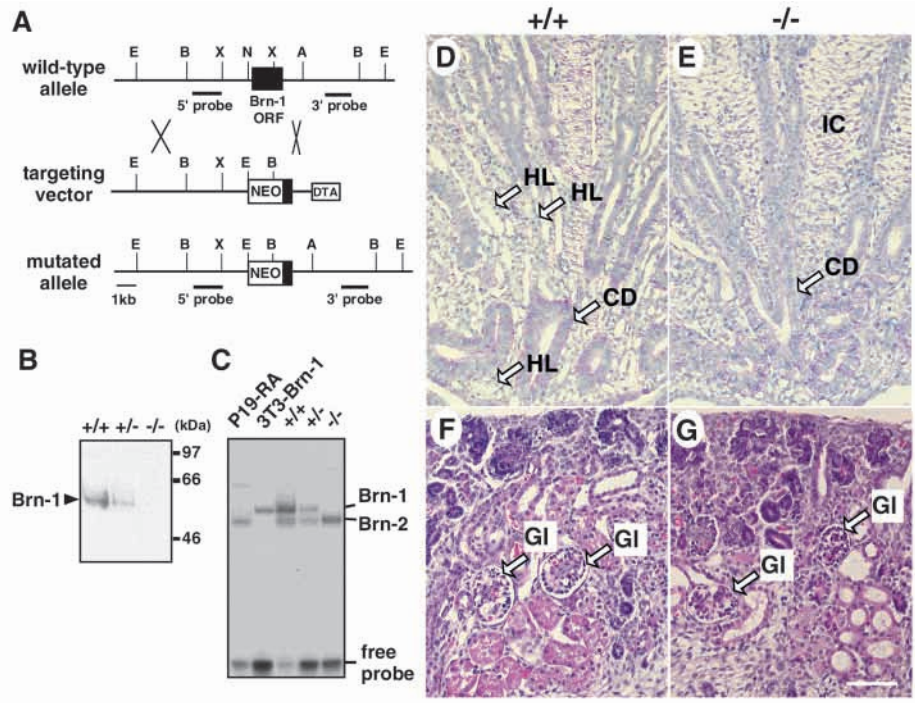

Fig. 1. Generation of *Brn1* knockout mice and histological changes in their kidneys at birth. (A) Representation of the wild-type allele, targeting vector and targeted allele of *Brn1*. The *Brn1* open reading frame is shown as a black box. The locations of the external 3′ and internal 5′ probes are indicated. NEO, neomycin-resistance gene driven by phosphoglycerate kinase gene promoter; DTA, diphtheria toxin A-chain gene; E, *Eco*RI; B, *Bam*HI; X, *Xho*I; N, *Not*I; A, *Apa*I. (B) Western blot analysis of kidney extracts from newborn *Brn1* mutants. The specific band of Brn1 detected by a polyclonal antiserum is reduced in *Brn1*$^{+/-}$ mice and absent from *Brn1*$^{-/-}$ mice. (C) Electrophoresis mobility-shift assay (EMSA) using brain extracts derived from newborn *Brn1* mutants. Cell extracts of *Brn1*-transfected NIH 3T3 cells (3T3-*Brn1*) served as a Brn1 protein control. Lysates of P19 cells treated with retinoic acid (P19-RA) were used as a Brn2 protein-positive control. (D,E) Staining of the kidney medulla derived from *Brn1*$^{+/+}$ (D) and *Brn1*$^{-/-}$ (E) mice with Hematoxylin and periodic acid-Schiff (PAS). The collecting ducts (CD) in *Brn1*$^{-/-}$ kidneys are comparable with those of the *Brn1*$^{+/+}$ kidney. The lops of Henle (HL), however, are absent from the *Brn1*$^{-/-}$ kidney. Interstitial cells (IC) are prominent in the *Brn1*$^{-/-}$ kidney in comparison with the wild-type kidney. (F,G) Cortices of *Brn1*$^{+/+}$ (F) and *Brn1*$^{-/-}$ (G) kidneys stained with Hematoxylin and Eosin. No significant differences in cortex morphology were observed between *Brn1*$^{+/+}$ and *Brn1*$^{-/-}$ kidneys. Gl, glomerulus. Scale bar: 50 μm.

mutants, suggesting that there was no loss of *Brn1*$^{-/-}$ mutants in utero. Absence of the Brn1 gene product in *Brn1*$^{-/-}$ mice was confirmed by western blot analysis (Fig. 1B) and electrophoresis mobility shift assay (EMSA) (Fig. 1C). *Brn1*$^{-/-}$ pups were indistinguishable from normal littermates and there was no significant difference in body weight at birth (Table 1). However, most died within 36 hours, with none surviving for more than 48 hours. Dissection of the *Brn1*$^{-/-}$ mice 2 hours after birth revealed significantly lower urine volumes compared with those measured in the *Brn1*$^{+/+}$ or *Brn1*$^{+/-}$ mice. This prompted us to analyze kidney function in these mice. The blood urea nitrogen (BUN) and potassium (K) levels in the sera of the *Brn1*$^{-/-}$ mice were significantly higher than in the sera of either the *Brn1*$^{+/+}$ or *Brn1*$^{+/-}$ mice (Table 1). These data indicate that renal dysfunction may contribute to the premature death of *Brn1*$^{-/-}$ mice.

At postnatal day 0 (P0), *Brn1*$^{-/-}$ kidneys were ~20% less in weight than those of either *Brn1*$^{+/+}$ or *Brn1*$^{+/-}$ mice (Table 1), suggesting a hypoplasticity of the *Brn1*$^{-/-}$ kidneys. Histological analyses showed equivalent numbers of collecting ducts (CDs) in the medulla region of both *Brn1*$^{+/+}$ and *Brn1*$^{-/-}$ kidneys (Fig. 1D,E, data not shown). PAS staining, however, revealed drastically reduced numbers of HLs in the kidneys of *Brn1*$^{-/-}$ mice (Fig. 1D,E). In addition, the areas occupied by interstitial cells between the CDs were more prominent in *Brn1*$^{-/-}$ kidneys, consistent with the HLs being replaced by these cells (Fig. 1D,E). By contrast, no remarkable changes were observed in the cortices of *Brn1*$^{-/-}$ kidneys (Fig. 1F,G). The number of glomeruli and the extent of their maturation in the kidneys of *Brn1*$^{-/-}$ mice were not significantly different from those of *Brn1*$^{+/+}$ or *Brn1*$^{+/-}$ mice (Table 1). In addition, there was no significant difference in proximal tubule number between the *Brn1* mutant mice (data not shown), although these numbers were difficult to quantitate.

Table 1. Developmental status and function of kidneys in newborn *Brn1* mutant mice

	Genotype		
	+/+	+/–	–/–
Body weight (g)	1.54±0.07	1.56±0.03	1.40±0.03
Kidney weight (g)	0.015±0.001	0.015±0.001	0.012±0.001†
BUN (serum) (mg/dl)	26.7±1.7	26.9±1.1	44.2±4.2†
K (serum) (mEq/l)	4.8±0.1	5.2±0.1	7.2±0.8†
Numbers of glomeruli*	44.2±6.8	47.7±1.6	42.3±4.7
Glomerular maturity index	2.03±0.05	2.02±0.03	1.96±0.03

*Numbers of glomeruli were counted in the median longitudinal section.
†P<0.05 versus +/+ by t-test, following ANOVA.
Mean±s.e.m. (n≥6).

To determine the function of Brn1 in kidney development, we analyzed its expression during mouse development. Throughout the initial phases of kidney development, we could not identify any Brn1-immunoreactive cells in any part of the embryonic kidney. Brn1 expression was first identified in a spherical cyst (Fig. 2A,B), a region of the renal vesicle containing early epithelial cells transformed from the metanephric blastema. This cyst, through a series of invaginations and elongations, initiates nephrogenesis to generate first comma-shaped and then S-shaped bodies (Kuure et al., 2000; Schedl and Hastie, 2000). Brn1 was specifically detected in the prospective HL, DCT and the MD within S-shaped bodies (Fig. 2C,D). During a subsequent stage in the development of these bodies into mature nephrons, Brn1 was detected within the developing HL, DCT and MD, but not in

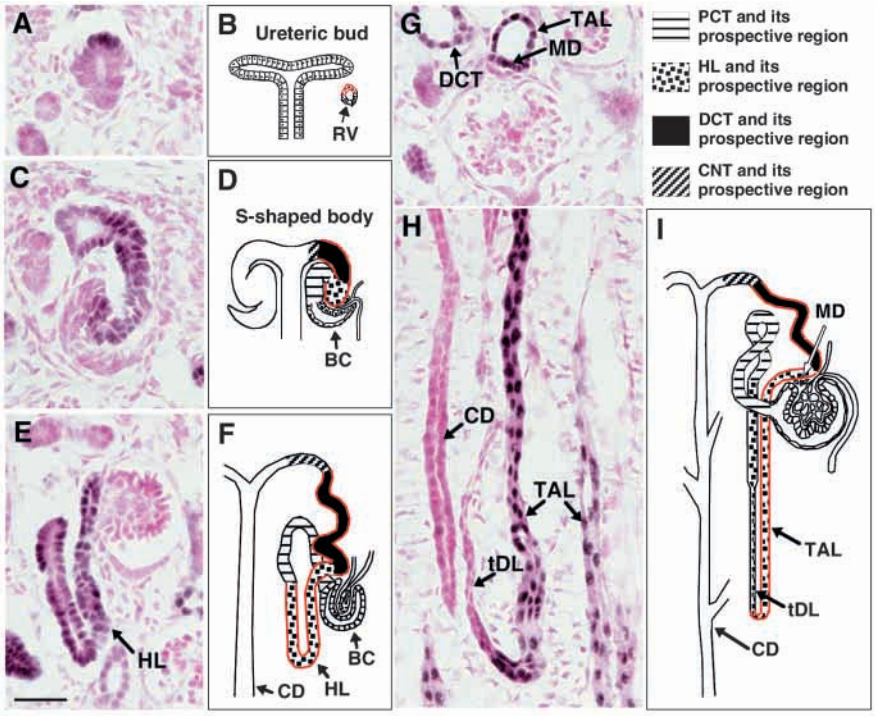

Fig. 2. Brn1 is expressed in the developing loop of Henle (HL) and distal convoluted tubule (DCT) during nephrogenesis. Brn1 immunostaining (A,C,E,G,H) and schematic drawings of the key stages of nephron development (B,D,F,I). Brn1 immunoreactivity is present in sections of the renal vesicle (RV; A,B); within the prospective HL, the DCT and the macula densa of nascent S-shaped bodies (C,D); within the elongating HL (E,F); and within the thick ascending limb (TAL), macula densa (MD) and DCT (G-I) of the newborn kidney. Brn1-positive region of the nephron are indicated by a red outline in the schematic drawings (B,D,F,I). RV, renal vesicle; BC, Bowman's capsule; PCT, proximal convoluted tubule; CNT, connecting tubule; tDL, thin descending limb. Scale bar: 20 μm. (B,D,F,I) Modified, with permission, from Fischer et al. (Fischer et al., 1995).

the glomerulus, proximal tubule or CD (Fig. 2E,F). In mature nephrons, Brn1 expression endured in the MD and DCT, but became regionalized to the TAL in HL (Fig. 2G-I). This expression pattern persisted through adulthood.

Elongation of HLs was severely retarded in homozygous *Brn1*-mutant mice

The expression of Brn1 in the developing HL prompted us to analyze HL development in *Brn1*$^{-/-}$ mutant mice. Nephrogenesis occurs continuously in the peripheral region of the kidney beginning at embryonic day 12.5 (E12.5) and lasting until P7-10 (Potter, 1972). Thus, newer nephrons are sequentially added to the nephrogenic zone, the outer region of the cortex beneath the renal capsule, while older nephrons move into deeper regions of the cortex with elongating HLs extending toward the medulla. Three distinct stages of developing HL were observed in the wild-type mouse kidney at E16.5, similar to the same stages in rat (Neiss, 1982). The first stage, the anlage, is a U-shaped structure located in the nephrogenic zone (Fig. 3A,D). The next stage, the primitive loop, elongates through the boundary of the cortex and medulla, with a bend lying within the medullary ray or outer medulla (Fig. 3B,D). In both stages, HLs contain cuboidal epithelial cells undergoing multiple mitoses. HLs in these stages were also observed within the *Brn1*$^{-/-}$ kidney at E16.5. In wild-type mice, we detected immature loops, the third stage of the developing HL. These loops possess a dilated tubule lumen and a morphologically differentiated tubule epithelium (Fig. 3C,D). Some bends in these immature loops reach almost to the papillary tip, the innermost region of the kidney. Cytologically, the descending limb of the immature loop displays a darkly stained thin epithelium. By contrast, the ascending limb of the immature loop contains lightly stained, tall cuboidal epithelial cells (Fig. 3C), defining the differentiation and proliferation of tubular epithelial cells that characterizes the immature loop differentiation stage. We could not detect any immature loops within the *Brn1*$^{-/-}$ kidney, despite an extensive analysis. To confirm this observation, we quantitated the developing HLs in *Brn1* mutant kidneys at E16.5 (Fig. 3E,F). This analysis confirmed the absence of immature loops in *Brn1*$^{-/-}$ kidneys (Fig. 3F). The number of primitive loops in *Brn1*$^{-/-}$ kidneys was twice that found in either *Brn1*$^{+/+}$ or *Brn1*$^{+/-}$ kidneys (Fig. 3E). This proportion remained true for mice at E17.5 or P0 (data not shown). We concluded that HL development was either perturbed or severely retarded at the primitive loop stage in *Brn1*-deficient kidneys.

To clarify the mechanism inhibiting primitive loop development in *Brn1*$^{-/-}$ kidneys, we examined cell proliferation within elongating HL by bromodeoxyuridine (BrdU) labeling at E16.5, the time point at which immature HLs first appear in *Brn1*$^{+/+}$ and *Brn1*$^{+/-}$ mice. Within the HL anlage, we observed a similar extent of BrdU incorporation among the *Brn1* mutant kidneys (Fig. 3G-I). During the primitive loop stage, the amount of BrdU incorporation in *Brn1*$^{-/-}$ kidneys was significantly lower than that of *Brn1*$^{+/+}$ and *Brn1*$^{+/-}$ kidneys (Fig. 3J-L), indicating a reduction in cell proliferation within the primitive loops of *Brn1*$^{-/-}$ mice. These data demonstrate an essential role for Brn1 in tubular cell proliferation at the primitive loop stage of HL development. We next examined the possible involvement of apoptosis in the retarded development of HL in *Brn1*$^{-/-}$ mice by TUNEL assay (Fig. 3M-P). At birth, we found cells in wild-type mice undergoing apoptosis only at the bend of the immature loop (Fig. 3O arrow). This physiological apoptosis plays an essential role in the generation of the thin ascending limb of the mature HL, which first appears just after birth in rat kidneys (Kim et al., 1996). In *Brn1*$^{-/-}$ kidneys lacking immature loops (Fig. 3P), significant numbers of apoptotic cells were detected throughout the primitive loop bend (Fig. 3N, arrows).

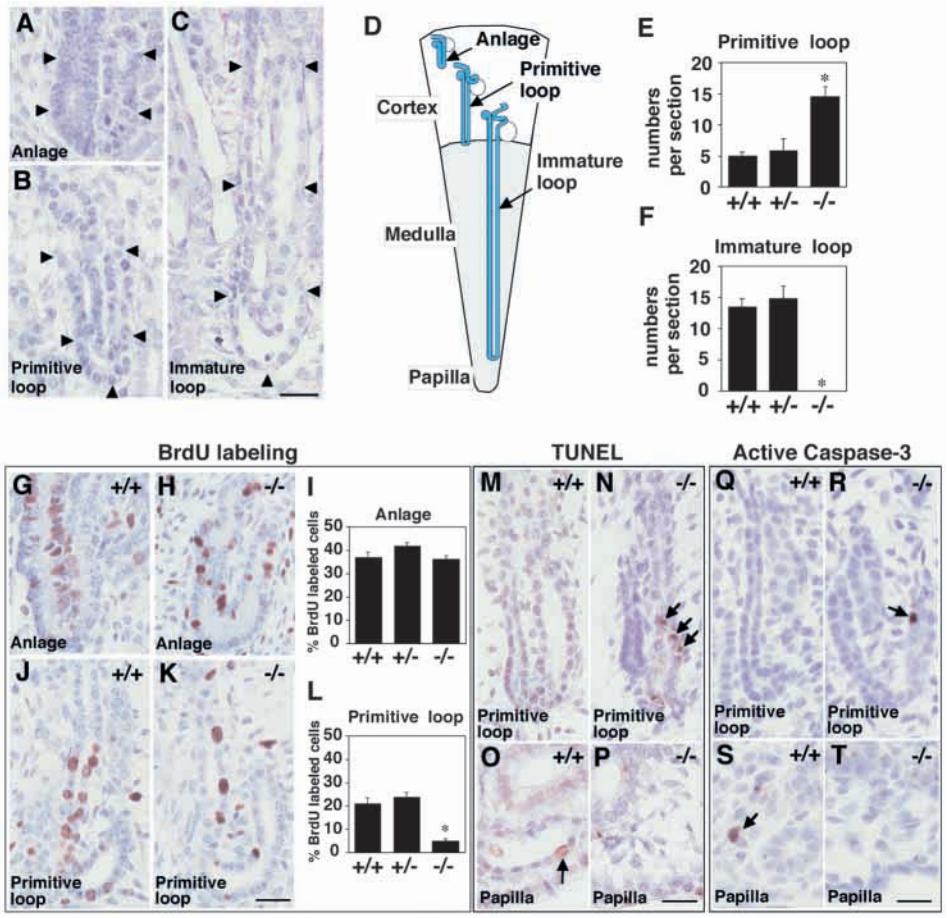

Fig. 3. Arrest of loop of Henle (HL) elongation at the primitive loop stage in *Brn1*-deficient kidney. (A-C) Classification of HL developmental stages; anlage (A), primitive loop (B) and immature loop (C). Each developing HL stage is outlined by arrowheads. (D) Schematic drawing of the anlage, primitive loop and immature loop of Henle. (E,F) Quantitation of the numbers of primitive loops and immature loops of Henle in *Brn1*-deficient kidneys. All observable independent HLs were counted within one median longitudinal section from each animal at E16.5. The number of primitive loops of Henle in $Brn1^{-/-}$ kidneys increased significantly from the levels seen in $Brn1^{+/+}$ kidneys (E). However, no immature loops of Henle were identified in $Brn1^{-/-}$ kidneys (F). Data are shown as the mean±s.e.m. (n=3 or 4). *P<0.05 compared with $Brn1^{+/+}$ kidney (ANOVA). (G-L) BrdU labeling in the anlage and primitive loops of Henle at E16.5. No significant difference in the numbers of BrdU-incorporated cells between $Brn1^{+/+}$ and $Brn1^{-/-}$ kidneys was detectable at the anlage stage (G-I). At the primitive loop stage, the number of cells incorporating BrdU was significantly decreased in $Brn1^{-/-}$ kidney in comparison with the $Brn1^{+/+}$ kidney (J-L). Data are shown as the mean±s.e.m. (n=3 or 4). *P<0.05 compared with $Brn1^{+/+}$ kidney (ANOVA). (M-P) TUNEL analysis of primitive and immature loops of Henle at P0. In the $Brn1^{+/+}$ kidney, TUNEL-positive cells were detected in the bend of the immature loop of Henle, near the papillary tip of medulla (O, arrow). TUNEL-positive cells were never observed in the primitive loop (M). In the $Brn1^{-/-}$ kidney, TUNEL-positive cells were present near the bend of primitive loop (N, arrows). The HL could not be identified in the papilla of $Brn1^{-/-}$ kidneys (P). (Q-T) Active caspase 3 immunostaining of primitive and immature loops of Henle at P0. In the $Brn1^{+/+}$ kidney, active caspase 3-positive cells were detected in the bend of the immature loop of Henle, near the papillary tip of medulla (S, arrow). Active caspase 3-positive cells were never observed in the primitive loop (Q). In the $Brn1^{-/-}$ kidney, active caspase 3-positive cells were present near the bend of primitive loop (R, arrow). The HL could not be identified in the papilla of $Brn1^{-/-}$ kidneys (T). Scale bars: 20 μm.

Apoptotic cells were never detected in this region of either $Brn1^{+/+}$ or $Brn1^{+/-}$ kidneys (Fig. 3M). To determine whether apoptosis observed in $Brn1^{+/+}$ immature loop and $Brn1^{-/-}$ primitive loop is associated with the activation of caspase cascade, we examined active caspase 3 expression by immunohistochemical analysis. Active caspase 3-positive cells were detected in almost the same manner to that observed by TUNEL assay described above (Fig. 3Q-T). This result suggests that apoptosis in both $Brn1^{+/+}$ immature loop and $Brn1^{-/-}$ primitive loop was induced through the activation of caspase cascade. We further examined the expressions of phosphorylated MAPK (ERK1/2) and anti-apoptotic protein Bcl2, both of which are known to suppress apoptosis. Their expressions were not detected in HLs throughout their developmental stages by immunohistochemical analysis. Therefore, we could not find any specific changes in their expressions for $Brn1^{+/+}$ immature loop and $Brn1^{-/-}$ primitive loop (data not shown). These results exclude the possible involvement of MAPK (ERK1/2) and Bcl2 in the apoptosis induction in $Brn1^{-/-}$ primitive loops or in the apoptosis suppression in $Brn1^{+/+}$ primitive loops. Taken together, Brn1 possibly suppresses apoptosis in primitive loop and, therefore, Brn1 deficiency may result in the premature induction of physiological apoptosis in primitive loop. Primitive loop apoptosis may at least in part contribute to the perturbation of HL development in $Brn1^{-/-}$ mice. These results support an essential role for Brn1 in the growth and survival of developing tubular epithelial cells.

Differentiation of HLs, MD and DCT is suppressed in $Brn1^{-/-}$ kidney

Although tubular epithelial cells within the wild-type primitive loop retain an immature appearance histologically, several molecular markers for HL are identifiable in the primitive loop, suggesting the initiation of differentiation. *Umod*, a gene that encodes a glycoprotein marker of the TAL (Bachmann et al., 1990), is first expressed in the anlage. *Ptger3*, a receptor for prostaglandin E_2 (Breyer et al., 1993), and *Nkcc2* (*Slc12a1*), a bumetanide-sensitive Na-K-2Cl co-transporter (Schmitt et al., 1999), begin to be expressed in the prospective TAL region of the primitive loop. In situ hybridization analysis of P0 kidney, however, failed to detect mRNA expression for any of these

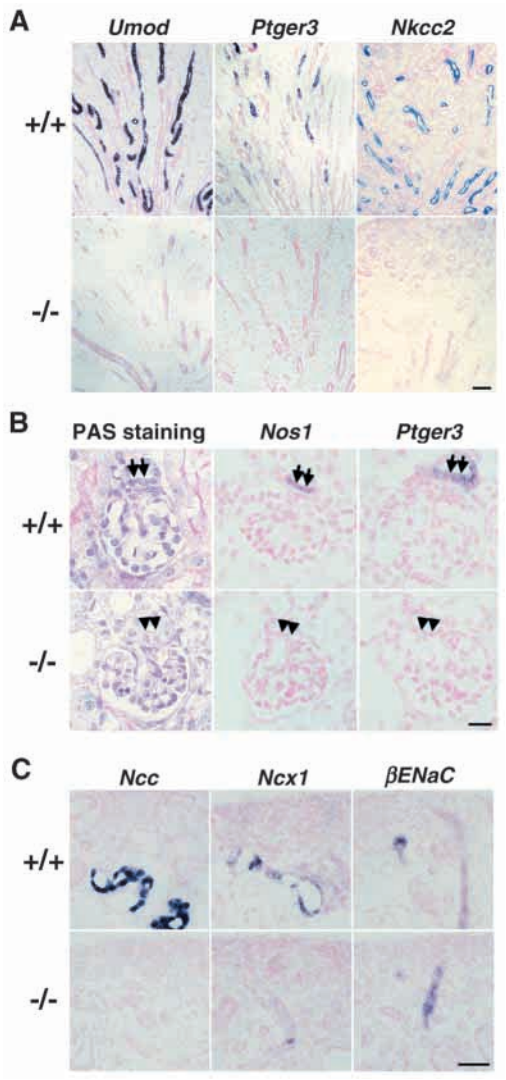

Fig. 4. Differentiation of the TAL, MD and DCT was impaired in the *Brn1*-deficient kidney. (A) In situ hybridization analyses of the TAL in newborn $Brn1^{+/+}$ and $Brn1^{-/-}$ kidneys. The expression of the Tamm-Horsfall glycoprotein gene (*Umod*), the prostaglandin E_2 receptor subtype EP_3 gene (*Ptger3*) and bumetanide-sensitive Na-K-2Cl co-transporter gene (*Nkcc2/Slc12a1*) was detected in the TAL of the $Brn1^{+/+}$, but not the $Brn1^{-/-}$ kidney, suggesting that TAL differentiation was impaired in Brn1-deficient animals. Scale bar: 50 μm. (B) Histological and in situ hybridization analyses of the MD and the surrounding TAL cells in $Brn1^{+/+}$ and $Brn1^{-/-}$ kidneys. PAS staining demonstrates that the MD in $Brn1^{+/+}$ kidneys (arrows) possesses the defining MD features; cells are crowded and protrude into the tubular lumen. The putative MD in $Brn1^{-/-}$ mice (arrowheads) does not display these features. Using in situ hybridization analysis, expression of the constitutive type 1 isoform of nitric oxide synthase gene (*Nos1*) was detected in the MD of the $Brn1^{+/+}$, but not the $Brn1^{-/-}$ kidney. *Ptger3* expression was detected in both the MD and the surrounding TAL cells of $Brn1^{+/+}$ kidney but was absent from the $Brn1^{-/-}$ kidney. Scale bar: 20 μm. (C) In situ hybridization analysis of DCT in $Brn1^{+/+}$ and $Brn1^{-/-}$ kidneys. The expression of the thiazide-sensitive Na-Cl co-transporter gene (*Ncc/Slc12a3*), a maker for DCT, was detected in $Brn1^{+/+}$ but not $Brn1^{-/-}$ kidneys. The expression of the Na/Ca exchanger gene (*Ncx1/Slc8a1*), a maker of the distal part of the DCT and for the CNT, was altered in $Brn1^{-/-}$ kidneys in comparison with that of $Brn1^{+/+}$ kidneys, suggesting that *Ncx1* expression in $Brn1^{-/-}$ kidneys remained only in the CNT. The expression of the amirolide-sensitive epithelial Na^+ channel gene (*βEnaC/Scnn1b*), a marker for CNT and CD, was indistinguishable in $Brn1^{+/+}$ kidney from that in $Brn1^{-/-}$ kidneys. Scale bars: 20 μm.

genes in the HL primitive loop in $Brn1^{-/-}$ mice (Fig. 4A). This observation was confirmed using RNase protection assays (RPA) of mRNA extracted from P0 $Brn1^{-/-}$ kidneys (see Fig. 6). These results suggest that differentiation of the HL primitive loop is perturbed in $Brn1^{-/-}$ mice. This differentiation defect may be independent from the defect in HL elongation described above. As *Umod* expression should be initiated in the anlage stage prior to the observation of any growth defects or induced apoptosis in $Brn1^{-/-}$ kidney, the lack of *Umod* expression suggests that the *Brn1* deficiency results in a far more complex developmental defect arising at the earlier stages of differentiation.

During nephrogenesis, Brn1 is also expressed in the MD and DCT and in the cell populations from which these regions arise (Fig. 2). The MD mediates tubulovascular signaling and renin secretion (Ito and Ren, 1993; Skott and Briggs, 1987), while the DCT facilitates the reabsorption of NaCl and Ca^{2+} (Bachmann and Kriz, 1998). We also examined the MD and DCT in *Brn1* mutant kidneys at P0, histologically and by in situ hybridization. In $Brn1^{+/+}$ and $Brn1^{+/-}$ kidneys, the MD, consisting of a plaque of columnar tubular cells protruding into the lumen within the cortical TAL of HL, was found adjacent to the hilus of the glomerulus (Fig. 4B). In $Brn1^{-/-}$ kidneys, however, the same cells did not exhibit any of the characteristic features of the MD. Instead, these cells displayed the same morphology as the surrounding cells (Fig. 4B). In situ hybridization of $Brn1^{-/-}$ nephrons, including the putative MD region, failed to detect expression of the constitutive type 1 isoform of the nitric oxide synthase gene (*Nos1*) or *Ptger3* (Fig. 4B), characteristic markers of MD cells (Breyer et al., 1993; Fischer et al., 1995). By immunohistochemical analysis, phosphorylated MAPK (ERK-1/2) was detected in macula densa and the surrounding cells in $Brn1^{+/+}$ kidney, but not in $Brn1^{-/-}$ kidney (data not shown). Electron microscopic analysis also failed to identify cells with any of the typical feature of MD cells, such as luminal microvilli or basal and lateral membrane foldings (Bachmann and Kriz, 1998; Fischer et al., 1995; Schmitt et al., 1999) (Fig. 5). These results suggest that the Brn1 deficiency also disrupted development of the MD. Interestingly, the morphology of the putative TAL, including the putative MD, in $Brn1^{-/-}$ kidneys differed from that of $Brn1^{+/+}$ and $Brn1^{+/-}$ TAL. The putative TAL of $Brn1^{-/-}$ kidneys retained the undifferentiated features of tubular cells, including simple cell membranes and small, sparse mitochondria with the cytoplasm (Fig. 5), supporting the observation that the differentiation of TAL cells is perturbed in $Brn1^{-/-}$ kidneys.

As it is difficult to identify the DCT in P0 kidneys histologically, we examined the expression of the thiazide-sensitive Na-Cl co-transporter gene, *Ncc*/*Slc12a3*, which is a specific marker of DCT cells (Schmitt et al., 1999). We detected *Ncc* expression by in situ hybridization in both $Brn1^{+/+}$ and $Brn1^{+/-}$ kidneys, but not in $Brn1^{-/-}$ kidneys (Fig. 4C). The Na/Ca exchanger gene, *Ncx1*/*Slc8a1* is normally

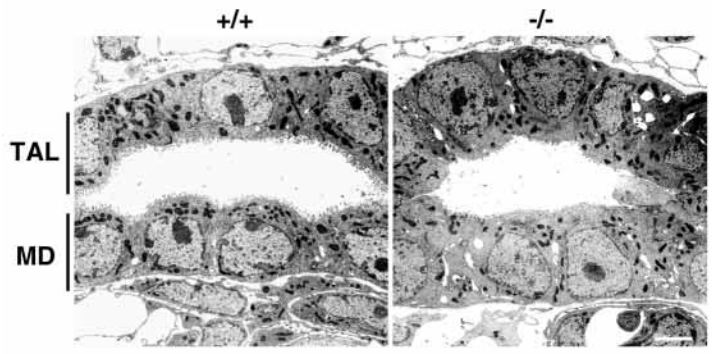

Fig. 5. Transmission electron micrographs of the MD and the surrounding TAL cells of *Brn1*$^{+/+}$ (left) and *Brn1*$^{-/-}$ (right) kidneys. MD cells of the *Brn1*$^{+/+}$ kidney exhibit characteristic features, including multiple luminal microvilli and basal and lateral membrane foldings. TAL cells of the *Brn1*$^{+/+}$ kidney display characteristic morphology, such as lateral extension, abundant microvilli, basal and lateral membrane foldings and cellular interdigitation. The putative TAL cells and MD cells of the *Brn1*$^{-/-}$ kidney are indistinguishable from each other, exhibiting immature morphology, including simple cell membranes, sparse luminal microvilli, and small and sparse mitochondria with the cytoplasm. Scale bar: 2 μm.

expressed in the distal region of the DCT and the connecting tubule (CNT) (Schmitt et al., 1999), a region of tubule that follows the DCT. In *Brn1*$^{-/-}$ kidneys, *Ncx1*/*Slc8a1* expression differed from that observed in *Brn1*$^{+/+}$ or *Brn1*$^{+/-}$ kidneys (Fig. 4C). The development of CNT appeared normal in *Brn1*$^{-/-}$ kidneys, as judged by the expression pattern of the amiloride-sensitive epithelial Na^+ channel gene, *βEnaC*/*Scnn1b*, which is a marker for CNT and CD (Schmitt et al., 1999). The pattern was indistinguishable from that of *Brn1*$^{+/+}$ or *Brn1*$^{+/-}$ kidneys (Fig. 4C). These results show that the expression of several molecules essential for DCT function was reduced in the *Brn1*$^{-/-}$ kidney. Electron microscopic analysis also demonstrated that there were some immature cells in the DCT region of *Brn1*$^{-/-}$ kidneys, which were not present in either *Brn1*$^{+/+}$ or *Brn1*$^{+/-}$ kidneys (data not shown). Together, these data suggest that the differentiation of DCT cells is perturbed by a deficiency in Brn1.

Expression levels of *Umod*, *Ptger3*, *Nkcc2*, *Kcnj1* and *Bsnd* were significantly reduced in the TAL of HLs of *Brn1*$^{+/-}$ kidneys

In mature nephrons, Brn1 expression in the HLs was regionalized within the TAL region (Fig. 2H,I). RPA analysis of mRNA extracted from *Brn1*$^{-/-}$ kidneys at P0 indicated a drastic reduction in the expression of several genes that are normally expressed in the TAL (Fig. 6), confirming the differentiation defect of HL. Interestingly, this analysis also demonstrated significant reductions in the expression levels of *Umod*, *Ptger3*, *Nkcc2*, *Kcnj1* (encoding an apical K^+ channel) (Simon and Lifton, 1998) and *Bsnd* (encoding a basolateral Cl^- channel β-subunit) (Birkenhager et al., 2001; Estevez et al., 2001) in *Brn1*$^{+/-}$ kidneys at P0 (Fig. 6). Morphologically, these kidneys were unaltered. We also identified significant reductions in the expression of these genes in *Brn1*$^{+/-}$ adult kidneys (Fig. 6), in which Brn1 expression within the TAL is half of that in wild-type kidneys (data not shown). *Nkcc2*, *Kcnj1* and *Bsnd* are essential for the reabsorption of NaCl by TAL cells (Birkenhager et al., 2001; Estevez et al., 2001; Simon and Lifton, 1998; Takahashi et al., 2000), which is a necessary step in hypertonic urine generation as it establishes a countercurrent multiplier system (Greger, 1985). We therefore wanted to examine kidney function in the adult *Brn1*$^{+/-}$ mice. Blood data (BUN, creatinine, Na^+, K^+, Cl^- and osmolality) and urine data (osmolality and daily urine volume) in *Brn1*$^{+/-}$ mice under euhydrated conditions were indistinguishable from that of wild-type mice (data not shown). In addition, neither urine osmolality 2 hours after intraperitoneal injection of dDAVP (1-desamino-8-D-arginine-vasopressin; 0.4 μg kg^{-1}) nor percent body weight loss after 24 hours water deprivation revealed any significant difference in the two genotypes (data not shown). Therefore, it was clear that adult *Brn1*$^{+/-}$ mice retain sufficient kidney function to generate hypertonic urine that is indistinguishable from that of wild-type mice. These results suggest that TAL cells in the *Brn1*$^{+/-}$ kidney are functionally normal and the significant reduction in gene expression may not result from a general dysfunction of TAL cells. Therefore, the Brn1 gene dosage effects on the expression levels of functionally essential TAL genes imply that Brn1 is essential for TAL function by activating the expression of these genes.

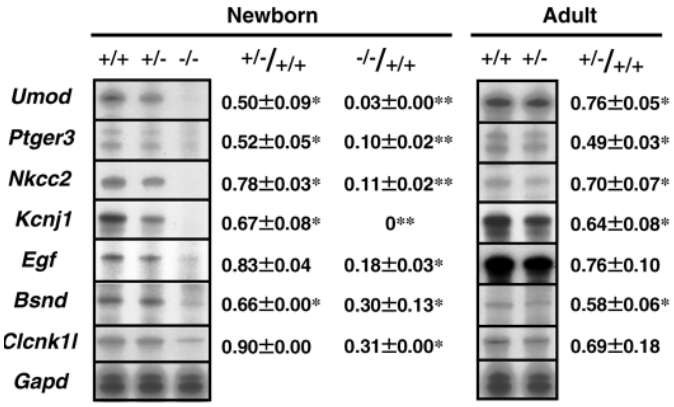

Fig. 6. Brn1 gene dosage effects on gene expression levels in *Brn1* mutant kidneys. We performed an RNase protection assay (RPA) using total RNA from newborn and adult kidneys. The expression of *Umod*, *Ptger3*, *Nkcc2* and *Kcnj1* (encoding apical K^+ channel) were nearly undetectable in the kidneys of newborn *Brn1*$^{-/-}$ mice. The mRNA level of epidermal growth factor (*Egf*) in the *Brn1*$^{-/-}$ kidney was reduced to ~20% to that of the wild type in newborn. The mRNA levels of the basolateral TAL Cl^- channel (*Clcnk1l*) and its β-subunit (*Bsnd*) in the *Brn1*$^{-/-}$ kidney were reduced to about 30% of wild-type levels in newborn. The mRNA levels of *Nkcc2*, *Bsnd* and *Kcnj1*, indispensable regulators of Na^+ reabsorption, were significantly reduced in *Brn1*$^{+/-}$ kidneys in comparison with the levels of *Brn1*$^{+/+}$ kidney in both newborn and adult kidneys. The mRNA levels of *Umod* and *Ptger3* in *Brn1*$^{+/-}$ kidneys were also significantly reduced in comparison with *Brn1*$^{+/+}$ kidneys. The mean values and s.e.m. of the ratios of the mutant to the wild-type signals are displayed at the right of the protected band patterns (n=3-4). All data were normalized to the *Gapd* signal prior to statistical analysis. *P<0.05, **P<0.001 compared with *Brn1*$^{+/+}$ kidney (ANOVA).

Discussion

In this study, we demonstrated the essential role of Brn1 in the development of HL, DCT and MD within the mouse kidney. Development of *Brn1*$^{-/-}$ HLs was retarded at primitive loop stage, which may be due to a reduction in cell proliferation and induction of apoptosis. We showed that this apoptosis in *Brn1*$^{-/-}$ primitive loop and physiological apoptosis in *Brn1*$^{+/+}$ immature loop are associated with the activation of caspase cascade. Therefore, it is conceivable that Brn1 possibly suppresses apoptosis in primitive loop and Brn1 deficiency may result in premature induction of physiological apoptosis.

The HL of a nephron is a unique structure that enables the generation of hypertonic urine, a function unique to birds and mammals (Casotti et al., 2000). Brn1, however, is also expressed in fish (zebrafish), suggesting that Brn1 pre-dates the establishment of HLs phylogenetically. Brn1 might have functioned originally in the development of DCT in fish, then the gene may have acquired an additional function to support HL development in birds and mammals. We recently showed that Brn1 functions in the development of neocortical neurons in mice (Sugitani et al., 2002). Because of the functional complementation between Brn1 and Brn2 during neocortical development, *Brn1*$^{-/-}$ mutant mice may exhibit a severe phenotype only within the kidneys, where Brn1 is the only class III POU factor expressed during development (He et al., 1989). The mode of Brn1 function in developing neocortical neurons is similar to its function in HL development, as Brn1 functions in both the proliferation and differentiation of precursors in both situations. In addition, Brn1 commonly plays an essential role in later phases of the developmental process (McEvilly et al., 2002; Sugitani et al., 2002). Nephrons require Brn1 function mainly during late development. The molecular pathways activated downstream of Brn1, however, are quite different between these two systems. In contrast to the activation of TAL-specific genes in developing HLs, Brn1 activates Dab1-dependent positioning processes in neocortical neurons (Sugitani et al., 2002). Therefore, the involvement of an additional molecule(s) specifying the pathways downstream of Brn1 is likely. Identification of such factors would aid our understanding of the molecular mechanisms underlying HL development.

We also elucidated an essential role of Brn1 in the nephron function in this study. The involvement of Brn1 in the regulation of gene expression in TAL of HLs was clearly shown by the significant reductions in the expression levels of *Umod*, *Ptger3*, *Nkcc2*, *Kcnj1* and *Bsnd* in *Brn1*$^{+/-}$ kidneys. As neither histological abnormality nor nephron dysfunction was observed in *Brn1*$^{+/-}$ kidneys as described above, expression levels of these genes in *Brn1*$^{+/-}$ kidneys seemed to be sufficient to support the development and function of HLs. Among these genes, *Nkcc2*, *Kcnj1* and *Bsnd* are essential for the reabsorption of NaCl by TAL cells (Birkenhager et al., 2001; Estevez et al., 2001; Simon and Lifton, 1998; Takahashi et al., 2000), which is a necessary step in hypertonic urine generation as it establishes a countercurrent multiplier system (Greger, 1985). Furthermore, their mutations have been shown to cause 'Bartter's syndrome', which describes a set of autosomal recessively inherited renal tubular disorders characterized by polyuria with hypokalemia and metabolic alkalosis (Birkenhager et al., 2001; Estevez et al., 2001; Simon and Lifton, 1998; Takahashi et al., 2000). Therefore, the involvement of *Brn1* mutations in these individuals should also be analyzed in the next study.

We thank Dr N. Yamanaka for his helpful advice on the histological analyses.

References

Bachmann, S., Metzger, R. and Bunnemann, B. (1990). Tamm-Horsfall protein-mRNA synthesis is localized to the thick ascending limb of Henle's loop in rat kidney. *Histochemistry* **94**, 517-523.

Bachmann, S. and Kriz, W. (1998). Histology, cytology, ultrastructure. In *Urinary System* (ed. T. C. Jones, G.C.H., U. Mmohr), pp. 3-36. Berlin: Springer Verlag.

Birkenhager, R., Otto, E., Schurmann, M. J., Vollmer, M., Ruf, E. M., Maier, L. I., Beekmann, F., Fekete, A., Omran, H., Feldmann, D. et al. (2001). Mutation of BSND causes Bartter syndrome with sensorineural deafness and kidney failure. *Nat. Genet.* **29**, 310-314.

Breyer, M. D., Jacobson, H. R., Davis, L. S. and Breyer, R. M. (1993). In situ hybridization and localization of mRNA for the rabbit prostaglandin EP3 receptor. *Kidney Int.* **44**, 1372-1378.

Casotti, G., Lindberg, K. K. and Braun, E. J. (2000). Functional morphology of the avian medullary cone. *Am. J. Physiol. Regul. Integr. Comp. Physiol.* **279**, R1722-1730.

Estevez, R., Boettger, T., Stein, V., Birkenhager, R., Otto, E., Hildebrandt, F. and Jentsch, T. J. (2001). Barttin is a Cl^- channel beta-subunit crucial for renal Cl^- reabsorption and inner ear K^+ secretion. *Nature* **414**, 558-561.

Fischer, E., Schnermann, J., Briggs, J. P., Kriz, W., Ronco, P. M. and Bachmann, S. (1995). Ontogeny of NO synthase and renin in juxtaglomerular apparatus of rat kidneys. *Am. J. Physiol.* **268**, F1164-1176.

Greger, R. (1985). Ion transport mechanisms in thick ascending limb of Henle's loop of mammalian nephron. *Physiol. Rev.* **65**, 760-797.

He, X., Treacy, M. N., Simmons, D. M., Ingraham, H. A., Swanson, L. W. and Rosenfeld, M. G. (1989). Expression of a large family of POU-domain regulatory genes in mammalian brain development. *Nature* **340**, 35-41.

Ito, S. and Ren, Y. (1993). Evidence for the role of nitric oxide in macula densa control of glomerular hemodynamics. *J. Clin. Invest.* **92**, 1093-1098.

Kim, J., Lee, G. S., Tisher, C. C. and Madsen, K. M. (1996). Role of apoptosis in development of the ascending thin limb of the loop of Henle in rat kidney. *Am. J. Physiol.* **271**, F831-845.

Kuure, S., Vuolteenaho, R. and Vainio, S. (2000). Kidney morphogenesis: cellular and molecular regulation. *Mech. Dev.* **92**, 31-45.

McEvilly, R. J., de Diaz, M. O., Schonemann, M. D., Hooshmand, F. and Rosenfeld, M. G. (2002). Transcriptional regulation of cortical neuron migration by POU domain factors. *Science* **295**, 1528-1532.

Minowa, O., Ikeda, K., Sugitani, Y., Oshima, T., Nakai, S., Katori, Y., Suzuki, M., Furukawa, M., Kawase, T., Zheng, Y. et al. (1999). Altered cochlear fibrocytes in a mouse model of DFN3 nonsyndromic deafness. *Science* **285**, 1408-1411.

Nakai, S., Kawano, H., Yudate, T., Nishi, M., Kuno, J., Nagata, A., Jishage, K., Hamada, H., Fujii, H., Kawamura, K. et al. (1995). The POU domain transcription factor Brn-2 is required for the determination of specific neuronal lineages in the hypothalamus of the mouse. *Genes Dev.* **9**, 3109-3121.

Neiss, W. F. (1982). Histogenesis of the loop of Henle in the rat kidney. *Anat. Embryol.* **164**, 315-330.

Niimura, F., Labosky, P. A., Kakuchi, J., Okubo, S., Yoshida, H., Oikawa, T., Ichiki, T., Naftilan, A. J., Fogo, A., Inagami, T. et al. (1995). Gene targeting in mice reveals a requirement for angiotensin in the development and maintenance of kidney morphology and growth factor regulation. *J. Clin. Invest.* **96**, 2947-2954.

Potter, E. L. (1972). *Normal and Abnormal Development of the Kidney*. Year Book Medical Publishers, Chicago.

Schedl, A. and Hastie, N. D. (2000). Cross-talk in kidney development. *Curr. Opin. Genet. Dev.* **10**, 543-549.

Schmitt, R., Ellison, D. H., Farman, N., Rossier, B. C., Reilly, R. F., Reeves, W. B., Oberbaumer, I., Tapp, R. and Bachmann, S. (1999). Developmental expression of sodium entry pathways in rat nephron. *Am. J. Physiol.* **276**, F367-381.

Simon, D. B. and Lifton, R. P. (1998). Mutations in Na(K)Cl transporters in Gitelman's and Bartter's syndromes. *Curr. Opin. Cell. Biol.* **10**, 450-454.

Skott, O. and Briggs, J. P. (1987). Direct demonstration of macula densa-mediated renin secretion. *Science* **237**, 1618-1620.

Sugitani, Y., Nakai, S., Minowa, O., Nishi, M., Jishage, K., Kawano, H., Mori, K., Ogawa, M. and Noda, T. (2002). Brn-1 and Brn-2 share crucial roles in the production and positioning of mouse neocortical neurons. *Genes Dev.* **16**, 1760-1765.

Takahashi, N., Chernavvsky, D. R., Gomez, R. A., Igarashi, P., Gitelman, H. J. and Smithies, O. (2000). Uncompensated polyuria in a mouse model of Bartter's syndrome. *Proc. Natl. Acad. Sci. USA* **97**, 5434-5439.

Yao, R., Ito, C., Natsume, Y., Sugitani, Y., Yamanaka, H., Kuretake, S., Yanagida, K., Sato, A., Toshimori, K. and Noda, T. (2002). Lack of acrosome formation in mice lacking a Golgi protein, GOPC. *Proc. Natl. Acad. Sci. USA* **99**, 11211-11216.